

Dual-Band Circularly Polarized Stacked Sapphire and TMM13i Rectangular DRA

Richa Gupta¹, Garima Bakshi^{2, *}, and Aakash Bansal³

Abstract—This paper documents a novel design of dual-band dielectric resonator antenna exhibiting circular polarization at a high-frequency band of (7.85 GHz–7.93 GHz) in addition to linearly polarized lower frequency band of (5.12 GHz–5.49 GHz) using new materials, sapphire, and TMM13i for antenna design. With sapphire and TMM13i being immune to physical change, the novel design is suitable for weather radar applications. The obtained circular polarization reduces signal attenuation. A four-layered structure with sapphire and TMM13i stacked alternatively with aperture coupled feed is presented. Additionally, the corners of the patch have been truncated, and a slot has been etched in order to obtain the dual-band resonance and circular polarization respectively. The design is simulated using Ansys HFSS and fabricated for measurements. The VSWR (Voltage standing wave ratio) is measured to be less than 2 for both the bands. The simulated and measured gains of the antenna are 5.2 dBi and 4.9 dBi, respectively.

1. INTRODUCTION

At the present age of wireless communication, the necessities for the antenna design are endless. There is a need for faster, dynamic, and broader bandwidth antennas with a minimized instrumentation size to meet the present-day wireless communication system needs. It may be a prime task to meet this demand in the related RF wireless domain considering that the design of the antenna has to be encapsulated into the wireless instrument. From the last few years for electronic equipment wireless applications, there has been an extensive investigation on two groups of antennas, i.e., microstrip antenna and dielectric resonator antenna (DRA). Over the past decade, many single point-fed circularly polarized (CP) DRAs with wide 3-dB Axial Ratio bandwidths have been presented in the literature.

By using better feeding techniques broadband CP DRAs have been achieved in [1, 2]. Wide CP bandwidths can also be attained with novel dielectric resonator (DR) structures [3–6]. Recently, a modified cross-slot excited hybrid CP DRA with a wide bandwidth of 24.6% has been presented in [7]. Because of frequent progressions in the new wireless communication systems, CP DRAs with dual-band performance are desired. Many such types of antennas have been developed in the past [8–13]. Dual-band antennas are typically accomplished by exciting the elemental and higher-order modes inside the DRA. In [9], the fundamental cylindrical DRA was excited by two feeding strips to comprehend dual-band CP operation, and wide bandwidths of 12.4% and 7.4% are achieved for the lower and higher bands, respectively. However, the dual-band couplers inside the design significantly increase the design complexity of the DRA. An individually fed dual-band DRA has been presented in [14] by introducing a diagonal groove at the top face and removing two opposite corners of the DRA. The modes of a rectangular DRA with a massive aspect ratio is also utilized to appreciate wide dual-band CP DRA, and measured bandwidths of 15.7% and 6.0% are obtained in [15]. However, the antenna documented

Received 27 January 2020, Accepted 6 April 2020, Scheduled 17 April 2020

* Corresponding author: Garima Bakshi (garima.bakshi31@yahoo.com).

¹ Maharaja Surajmal Institute of Technology, Delhi, India. ² School of Engineering & Technology, Ansal University, Gurgaon, India.

³ Wolfson School of Mechanical Electrical & Manufacturing Engineering, Loughborough University, UK.

encompasses a low antenna gain at the lower band, which might be caused by the fact that the radiation pattern of the mode is null within the broadside direction.

Some certain specific geometries of DRAs like conical, bi-conical, notch, triangle form, have shown to increase the impedance bandwidth [16, 17] for broadband DRA. It was displayed by an experiment in [18, 19] that heaping two DRAs one over the other can enhance the impedance bandwidth of the antenna. However, by this technique, the DRA's volume could be an important downside that cannot maintain the most important characteristic of low-profile and additionally its challenges in fabrication. Broader bandwidth is shown to be attained by piling-up two dissimilar microwave materials in A-shape using a P-shape parasitic strip [20–22]. It has been shown that broadband operation was achieved by stacking the triangular dielectric resonator antenna for wireless applications in 5–6 GHz frequency range by a conformal patch feeding technique [23–26]. Limited research work has been done on the sapphire-based antenna [27–29]. In this research work, a four-layer stacked rectangular dielectric resonator antenna (RDRA) with sapphire and TMM13i has been developed. It has been presented that the antenna size can also be easily varied by using the sapphire structure. The designed antenna has potential applications in next-generation mobile communications. It is accomplished using low-permittivity DRA volume put on high permittivity DRA volume. The antenna comprises dielectric constants of 10 and 12.8, heaped-up to acquire better bandwidth as matched to the conventional RDRA. Physical factors of stacked RDRA has been improved by extensive simulations using Ansoft HFSS. The novel design consists of a four-layered structure with sapphire and TMM13i stacked alternatively. A patch with corners truncated and slot etched is added to it in order to attain a dual-band and multiple polarizations, respectively.

2. ANTENNA CONFIGURATION

Figure 1 presents the suggested design for a stacked RDRA. The four DRA slabs (slab 1, 2, 3, and 4) as illustrated in Fig. 1 are made from different permittivities ϵ_{r1} and ϵ_{r2} with different cross-sectional

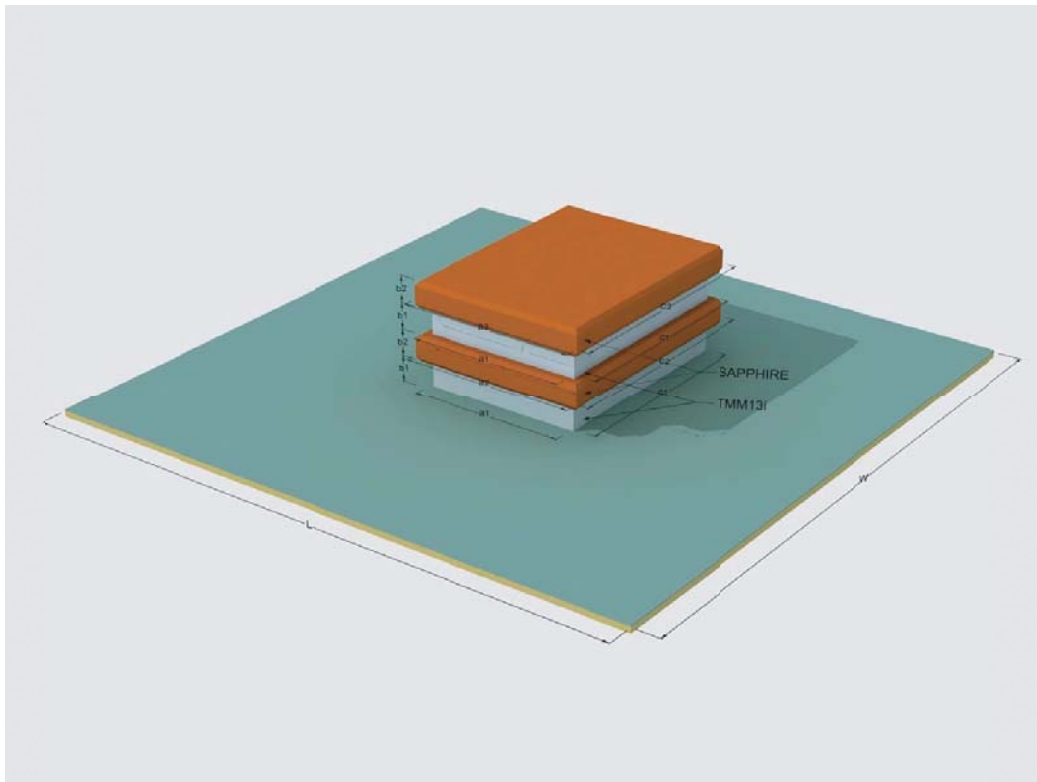


Figure 1. Stacked RDRA.

areas and different heights, h_1 and h_2 to form the stacked RDRA. Slab 1 (TMM13i) is placed above the microstrip line for coupling, whereas slab 2 (sapphire) is placed on the top of slab 1 for electromagnetic coupling followed by slab 3 (TMM13i) and slab 4 (sapphire). The total height of stacked RDRA is calculated to be $h = h_1 + h_2 + h_1 + h_2$. The stacked RDRA design is placed in the center of tan FR-4 epoxy substrate having a dielectric constant of 4.4, dimensions 50 mm mm, and a thickness of 0.8 mm. The sapphire and TMM13i used have dielectric constants of 10 and 12, and dimensions 10 mm mm.5 mm & 8 mm mm.5 mm, respectively. All the design dimensions are summarized in Table 1. In the designed antenna, circular polarization is attained by using two cross slots of equal lengths at 90 degrees to each other, to couple energy from aperture coupled microstrip line to RDRA. The dimensions of the feed line and slot etched from the ground plan are 1.2 mm mm and 1.5 mm.5 mm, respectively, as shown in Fig. 2. The patch beneath the RDRA is truncated, and two cross slots are cut to support circular polarization as shown in Fig. 3.

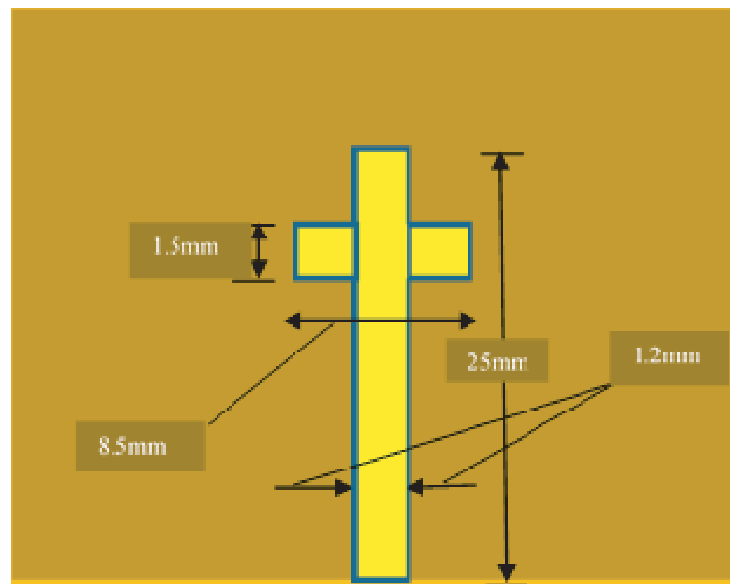


Figure 2. Aperture coupled feed (top view).

Table 1. Design dimensions of stacked RDRA.

S. No.	Element	Dimensions (mm)
1	Substrate	50 mm * 50 mm * 0.8 mm ($\epsilon_r = 4.4$)
2	Ground Plane	50 mm * 50 mm
3	Slab 1 (TMM13i RDRA)	8 mm × 12 mm × 2.5 mm ($\epsilon_r = 10$)
4	Slab 2 (Sapphire RDRA)	10 mm × 13 mm × 2.5 mm ($\epsilon_r = 12.8$)
5	Slab3 (TMM13i RDRA)	8 mm × 12 mm × 2.5 mm ($\epsilon_r = 10$)
6	Slab4 (Sapphire RDRA)	10 mm × 13 mm × 2.5 mm ($\epsilon_r = 12.8$)
7	Feedline	1.2 mm × 25 mm
8	Aperture Slot	1.5 mm × 8.5 mm
9	Patch	40 mm × 20 mm
10	Cross Slot	10 mm × 3 mm

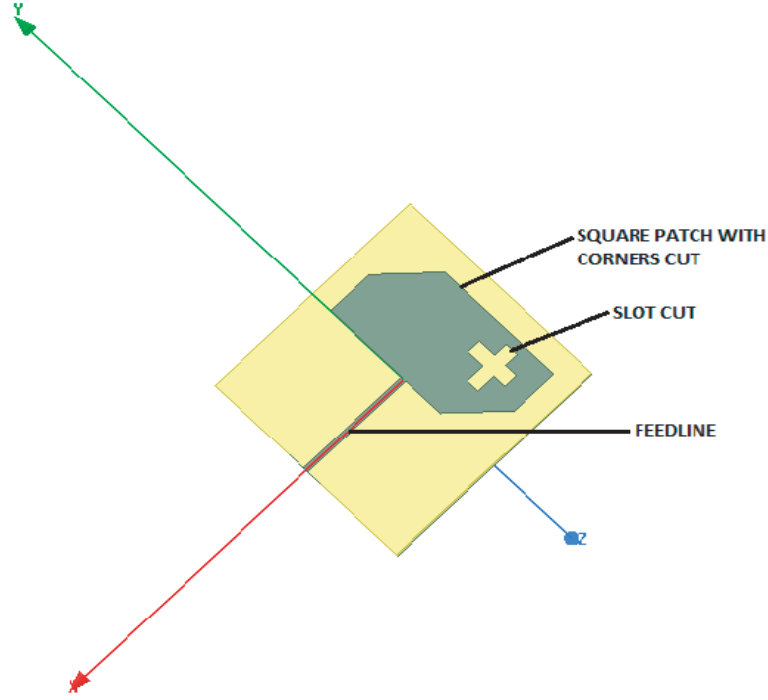


Figure 3. Proposed antenna design (front view).

3. DESIGN FORMULATION

The complete solution of propagation constant, i.e., k_x , k_y and k_z has been given by the transcendental equation of RDRA. Also, the mathematical analysis of the transcendental equation in rectangular RDRA has been derived [28].

$$k_x^2 + k_y^2 + k_z^2 = \varepsilon_r k_0^2 \quad (1)$$

$$f_0 = \frac{c}{2\pi\sqrt{\varepsilon_r}} \sqrt{k_x^2 + k_y^2 + k_z^2} \quad (2)$$

$$k_x = \frac{\pi}{a}; \quad k_y = \frac{\pi}{b} \quad (3)$$

$$k_z \left(\tan \frac{k_z d}{2} \right) = \sqrt{(\varepsilon_r - 1)k_0^2 - k_z^2} \quad (4)$$

where ε_r denotes the dielectric constant of dielectric resonator antenna; c is the velocity of light; and k_0 , k_x , k_y , and k_z are wavenumbers along x , y , and z directions, respectively. For the purpose of providing the excitation aperture coupled feed scheme has been employed.

Slot length of the antenna is defined using the equation,

$$L_S = \frac{0.4\lambda_0}{\sqrt{\varepsilon_e}} \quad (5)$$

where λ_0 is the wavelength, and the effective permittivity is defined as:

$$\varepsilon_e = \frac{\varepsilon_r + \varepsilon_s}{2} \quad (6)$$

where ε_r and ε_s are the dielectric constants of the rectangular dielectric resonator and substrate, respectively. The field equations are given below.

$$E_x = 0 \quad (7)$$

$$E_y = Ak_z \cos(k_x x) \cos(k_y y) \sin(k_z z) \quad (8)$$

$$E_z = -Ak_y \cos(k_x x) \sin(k_y y) \cos(k_z z) \tag{9}$$

$$H_y = \frac{k_x k_y}{j\omega\mu_0} A \sin(k_x x) \sin(k_y y) \cos(k_z z) \tag{10}$$

$$H_z = \frac{k_x k_z}{j\omega\mu_0} A \sin(k_x x) \sin(k_y y) \tag{11}$$

$$H_x = \frac{(k_z^2 + k_y^2)}{j\omega\mu_0} A \cos(k_x x) \cos(k_y y) \cos(k_z z) \tag{12}$$

4. ANTENNA DESIGN ANALYSIS

To exceed the apprehend of the design development process, three designed antennas are demonstrated in Figs. 4(a)–(c). The design of antenna 1 is made up of only stacked RDRA without any patch and slot etched. In antenna 2 design structure, there is a patch etched while in antenna 3 design structure, which is also the final structure, consists of the patch with corners truncated and slot etched in it. The simulations have been done for all three designs, and results are shown from Fig. 5 to Fig. 10. It can be seen from Fig. 5 that antenna 1 design without patch gives two bands without any circular polarization whereas antenna 2 with patch provides four bands with no circular polarization. The design of cross slots and truncated patch corners (Antenna 3) produces circular polarization. Table 2

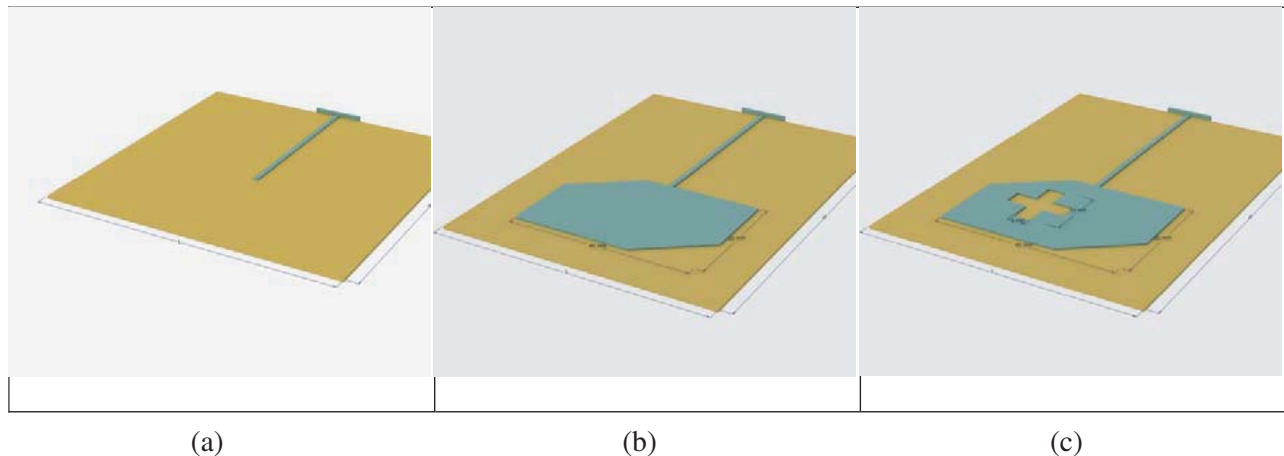


Figure 4. Development phases of the antenna structure. (a) Antenna 1. (b) Antenna 2. (c) Antenna 3.

Table 2. Comparison results of all three antenna design.

Antenna design	Frequency (GHz)	S ₁₁ (dB)	VSWR	Axial Ratio Bandwidth	Gain (dBi)
1	5.29–5.84 GHz (550 MHz)	–19 dB	1.2	-	5.4 dBi
	6.92–7.29 GHz (370 MHz)	–14 dB	1.4		
2	3.58–3.68 GHz (100 MHz)	–18 dB	1.3	-	5.3 dBi
	5.28–5.55 GHz (270 MHz)	–17 dB	1.35		
	6.76–6.95 GHz (190 MHz)	–12 dB	1.63		
3	7.73–8.02 GHz (290 MHz)	–19 dB	1.25	(7.84–7.92 GHz) (80 MHz)	5.2 dBi
	5.25–5.52 GHz (270 MHz)	–18 dB	1.35		
	7.47–7.95 GHz (480 MHz)	–23 dB	1.18		

shows all the performance comparisons of the three antennas discussed. As shown in Fig. 5 and Fig. 6, Antenna 1 exhibits dual 10 dB impedance bandwidths of (5.29–5.84 GHz) and (6.92–7.29 GHz) with no circular polarization while antenna 2 provides four regions of operation (3.58–3.68 GHz), (5.28–5.55 GHz), (6.76–6.95 GHz), and (7.73–8.02 GHz), respectively, but the axial ratio is not properly aligned in obtained band. Due to the truncated corner of patch and cross slot, antenna 3 provides dual 10 dB impedance bandwidths in the region (5.25–5.52 GHz) and (7.47–7.95 GHz), respectively, along with circular polarization in the region (7.84–7.92 GHz) as demonstrated in Fig. 5 and Fig. 6. The VSWR is less than 2 for the design of antenna 3 as demonstrated in in Fig. 9, showing a good impedance match. Thus, antenna 3 design structure provides dual-band resonance exhibiting linear polarization at a lower frequency band of (5.25 GHz–5.52 GHz) and circular polarization at a higher frequency band of (7.84 GHz–7.92 GHz), as can be interpreted from the axial ratio graph shown in Fig. 6. There is a slight change in gain performance of the three antennas as illustrated in Fig. 7. The H field distribution of the antenna is shown in Fig. 8.

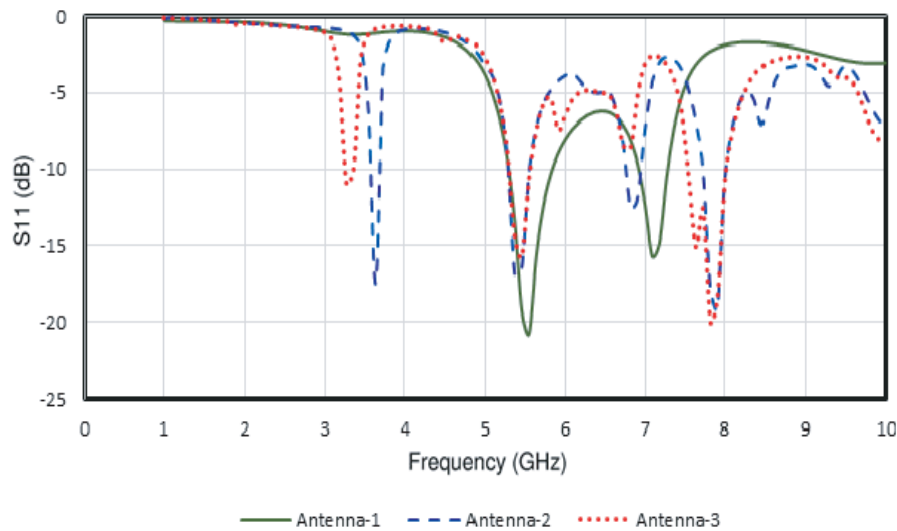


Figure 5. Reflection coefficient of antenna 1, antenna 2, antenna 3.

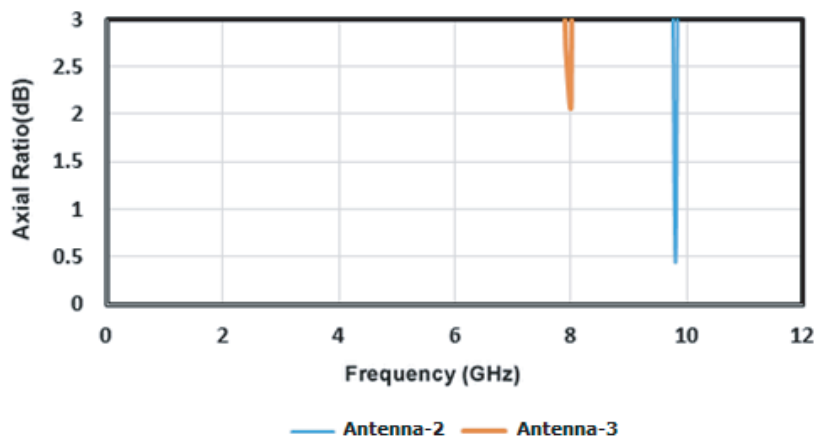


Figure 6. Axial ratio of antenna 2 and antenna 3.

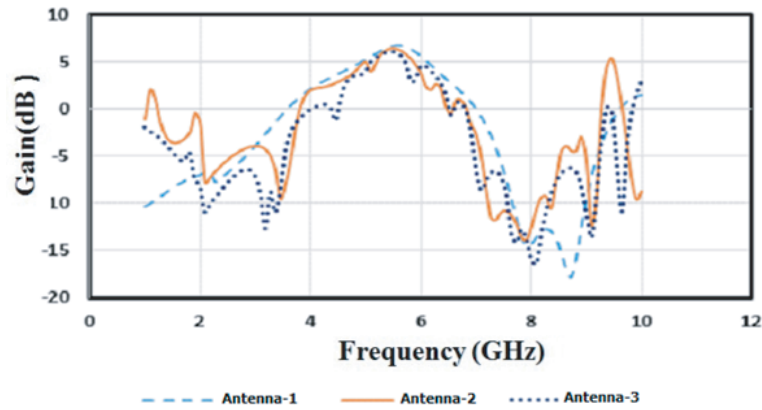


Figure 7. Gain of all three antenna structures.

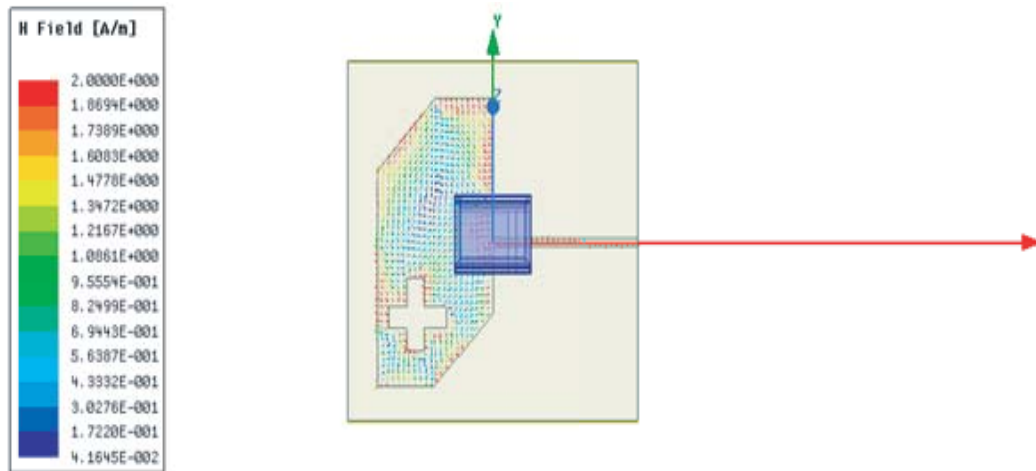


Figure 8. Circular polarization in antenna 3.

5. MEASURED RESULTS AND DISCUSSION

The proposed antenna 3 design is fabricated as per the parameters given in Table 1. Fig. 10 shows photographs of the fabricated antenna and experimental setup for the measurement of return loss characteristics of the antenna. The return loss characteristics of the antenna are measured using a Vector Network Analyzer. The measured return loss characteristics of the antenna are shown in Fig. 10. A comparison of measured and simulated performances of the proposed antenna is listed in Table 3.

Table 3. Comparison of simulated and measured antenna parameters.

Results	Frequency band (GHz)	Return loss S_{11} (dB)	10 dB Impedance bandwidth (MHz)	Axial Ratio bandwidth	Gain (dBi)
Simulated	5.25–5.52 GHz	–18 dB	270 MHz	(7.84–7.92 GHz)	5.2 dBi
	7.47–7.95 GHz	–23 dB	480 MHz	80 MHz	
Measured	5.12–5.49 GHz	–21 dB	370 MHz	(7.85–7.93 GHz)	4.9 dBi
	6.25–6.75 GHz	–20 dB	500 MHz	80 MHz	

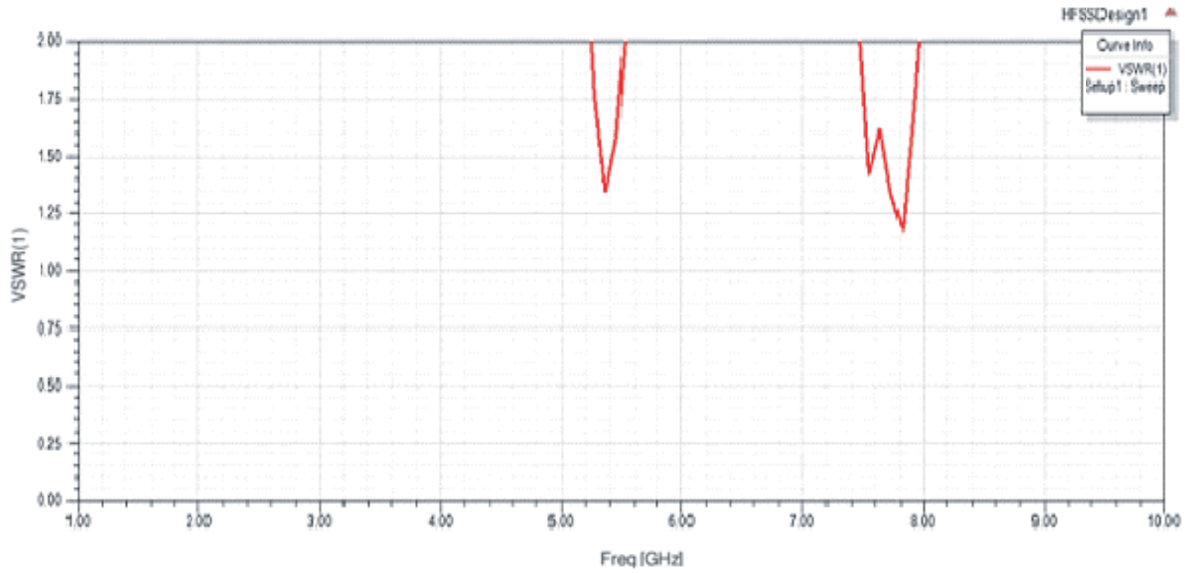
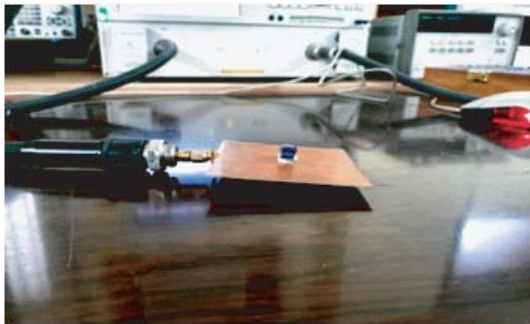
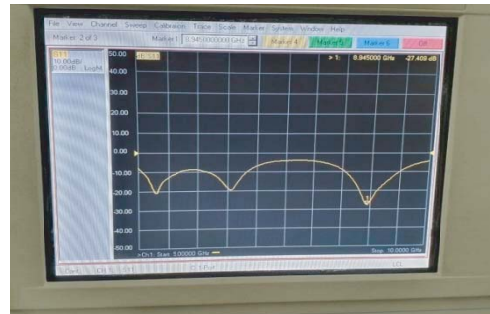


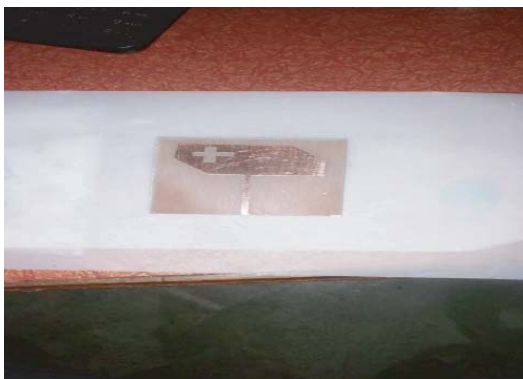
Figure 9. VSWR for antenna 3.



(a)



(b)



(c)



(d)

Figure 10. Experimental setup of antenna 3. (a) Prototype measurement. (b) VNA measurement. (c) Patch with slot and truncated corner. (d) Test setup.

The antenna has a measured 10-dB impedance bandwidth of 370 MHz (5.12–5.49 GHz) and 500 MHz (6.25–6.75 GHz). There is a slight shift in the frequency band in the fabricated antenna. The radiation patterns of the antenna are measured in an anechoic chamber. The experimental setup used for

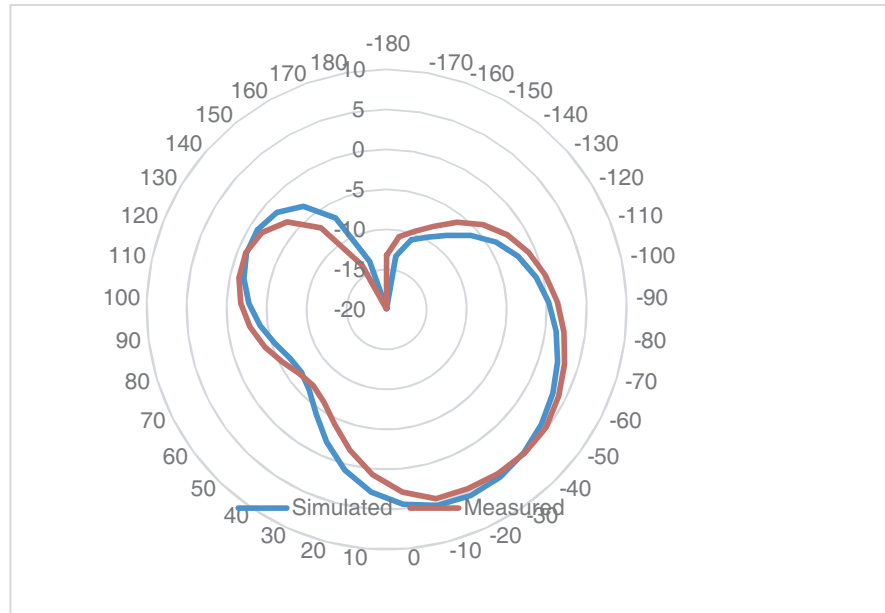


Figure 11. Measured radiation pattern of antenna 3.

measurements is Star lab with 18 GHz anechoic chamber. The standard horn antenna of frequency 18 GHz and gain 5 dBi is used inside the chamber to test the designed antenna. The radiation pattern of the antenna is shown in Fig. 11 and is presented to be broadside and stable in the required frequency range. The measured gain is 4.9 dBi which is slightly less than simulated gain due to fabrication losses.

Further, a comparison between past works presented in literature and the proposed design is presented in Table 4. It can be seen that the proposed structure presents a comparatively better result and higher gain. Also, the material used is resistant to temperature and physical climate change, making it a perfect candidate for weather radar applications [33–36].

Table 4. Comparison between proposed stacked design and past works presented in the literature.

DRA shape	Type of Excitation	Lower Band		Upper band		Gain (dBi)
		Operating Frequency (GHz)	Impedance Bandwidth (%)	Operating Frequency range (GHz)	Impedance Bandwidth %	
Rectangular [28]	Aperture Coupling	2.4–2.51	4.48	5.03–5.35	6.17	
Cylindrical [29]	CPW Feed	3.3–3.61	8.97	4.6–4.91	4.8	
Cylindrical [30]	Microstrip Line	2.36–2.5	3.3	5.4–5.8	5.7	
Stacked [31]	Aperture Coupling	6.79–7.27 GHz	6.82	-	-	5.2
Stacked [32]	Aperture Coupling	7.41–8.21	10.24	9.11–12.65	32.53	2.5
Proposed Stacked	Aperture Coupling	5.12–5.49 GHz	6.97	6.25–6.75	7.69	4.9

6. CONCLUSION

A novel design of a stacked rectangular dielectric resonator antenna (RDRA), made up of sapphire and TMM13i has been documented in this paper. At a low frequency band of (5.25 GHz–5.52 GHz), it exhibits linear polarization that can be used for wireless communication application. The design provides circular polarization at higher frequency band of (7.47 GHz–7.95 GHz). The circular polarization reduces signal attenuation and diminishes the adverse climatic conditions effects on signal.

REFERENCES

1. Sulaiman, M. I. and S. K. Khamas, "A singly fed wideband circularly polarized dielectric resonator antenna using concentric open-half-loops," *IEEE Antennas Wireless Propag. Lett.*, Vol. 10, 1305–1308, 2011.
2. Zou, M., J. Pan, Z. Nie, and P. Li, "A wideband circularly polarized rectangular dielectric resonator antenna excited by a lumped resistively loaded monofilar-spiral-slot," *IEEE Antennas Wireless Propag. Lett.*, Vol. 12, 1646–1649, 2013.
3. Lu, K., K. W. Leung, and Y. M. Pan, "Theory and experiment of the hollow rectangular dielectric resonator antenna," *IEEE Antennas Wireless Propag. Lett.*, Vol. 10, 631–634, 2011.
4. Pan, Y. M. and K. W. Leung, "Wideband circularly polarized trapezoidal dielectric resonator antenna," *IEEE Antennas Wireless Propag. Lett.*, Vol. 9, 588–591, 2010.
5. Pan, Y. M. and K. W. Leung, "Wideband omnidirectional circularly polarized dielectric resonator antenna with parasitic strips," *IEEE Transactions on Antennas and Propagation*, Vol. 60, No. 6, 2992–2997, Jun. 2012.
6. Wang, K. X. and H. Wong, "A circularly polarized antenna by using rotated-stair dielectric resonator," *IEEE Antennas Wireless Propag. Lett.*, Vol. 14, 787–790, 2015.
7. Zou, M. and J. Pan, "Wideband hybrid circularly polarized rectangular dielectric resonator antenna excited by modified cross-slot," *Electron. Lett.*, Vol. 50, No. 16, 1123–1125, Jul. 2014.
8. Ding, Y., K. W. Leung, and K. M. Luk, "Compact circularly polarized dualband zonal-slot/DRA hybrid antenna without external ground plane," *IEEE Transactions on Antennas and Propagation*, Vol. 59, No. 6, 2404–2409, Jun. 2011.
9. Fang, X. S. and K. W. Leung, "Linear-/circular-polarization designs of dual-/wide-band cylindrical dielectric resonator antennas," *IEEE Transactions on Antennas and Propagation*, Vol. 60, No. 6, 2662–2671, Jun. 2012.
10. Li, B., C. X. Hao, and X. Q. Sheng, "A dual-mode quadrature-fed wideband circularly polarized dielectric resonator antenna," *IEEE Antennas Wireless Propag. Lett.*, Vol. 8, 1036–1038, 2009.
11. Ngan, H. S., X. S. Fang, and K. W. Leung, "Design of dual-band circularly polarized dielectric resonator antenna using a higher-order mode," *Proc. IEEE-APS APWC*, 424–427, 2012.
12. Fang, X., K. W. Leung, and E. H. Lim, "Singly-fed dual-band circularly polarized dielectric resonator antenna," *IEEE Antennas Wireless Propag. Lett.*, Vol. 13, 995–998, 2014.
13. Zhang, M., B. Li, and X. Lv, "Cross-slot-coupled wide dual-band circularly polarized rectangular dielectric resonator antenna," *IEEE Antennas Wireless Propag. Lett.*, Vol. 13, 532–535, 2014.
14. Almpanis, G., C. Fumeaux, and R. Vahldieck, "Novel broadband dielectric resonator antenna fed through double-bowtie-slot excitation scheme," *ACES Journal*, Vol. 22, No. 1, 97–104, 2007.
15. Chair, R., A. A. Kishk, and K. F. Lee, "Wideband simple cylindrical dielectric resonator antenna," *IEEE Microwave and Wireless Components Letters*, Vol. 15, No. 4, 241–243, 2005.
16. Kishk, A. A., X. Zhang, A. W. Glisson, and D. Kajfez, "Numerical analysis of stacked dielectric resonator antennas excited by a coaxial probe for wideband application," *IEEE Transaction on Antenna and Propagation*, Vol. 51, No. 8, 1996–2006, 2003.
17. Rocha, H. H. B., F. N. A. Freire, R. S. T. M. Sohn, M. G. da Silva, M. R. P. Santos, C. C. M. Junqueira, T. Cordaro, and A. S. B. Sombra, "Bandwidth enhancement of stacked dielectric resonator antennas excited by a coaxial probe: an experiment and numerical investigation," *IET Microwave Antennas Propagation*, Vol. 2, No. 6, 580–587, 2008.

18. Khalajmehrabadi, A., M. K. A. Rahim, and M. Khalily, "Dual band double stacked dielectric resonator antenna with a P-shape parasitic strip for circular polarization," *IEEE International on RF and Microwave Conference (RFM)*, 444–447, 2011.
19. Coulibaly, Y., M. Nedil, L. Talbi, and T. A. Denidni, "Design of mm-wave broadband CPW-fed stacked dielectric resonator antenna for underground mining communication," *IEEE International Symposium on Antennas and Propagation Society*, 1–4, 2010.
20. Kumari, R., K. Parmar, and S. K. Behera, "Conformal patch fed stacked triangular dielectric resonator antenna for WLAN applications," *International Conference on Emerging Trends in Robotics and Communication Technologies (INTERACT)*, 104–107, 2010.
21. Almpanis, G., C. Fumeaux, and R. Vahldieck, "Novel broadband dielectric resonator antenna fed through double-bowtie-slot excitation scheme," *ACES Journal*, Vol. 22, No. 1, 97–104, 2007.
22. Chair, R., A. A. Kishk, and K. F. Lee, "Wideband simple cylindrical dielectric resonator antenna," *IEEE Microwave and Wireless Components Letters*, Vol. 15, No. 4, 241–243, 2005.
23. Kishk, A. A., X. Zhang, A. W. Glisson, and D. Kajfez, "Numerical analysis of stacked dielectric resonator antennas excited by a coaxial probe for wideband application," *IEEE Transactions on Antenna and Propagation*, Vol. 51, No. 8, 1996–2006, 2003.
24. Rocha, H. H. B., F. N. A. Freire, R. S. T. M. Sohn, M. G. da Silva, M. R. P. Santos, C. C. M. Junqueira, T. Cordaro, and A. S. B. Sombra, "Bandwidth enhancement of stacked dielectric resonator antennas excited by a coaxial probe: An experiment and numerical investigation," *IET Microwave Antennas Propagation*, Vol. 2, No. 6, 580–587, 2008.
25. Khalajmehrabadi, A., M. K. A. Rahim, and M. Khalily, "Dual band double stacked dielectric resonator antenna with a P-shape parasitic strip for circular polarization," *IEEE International on RF and Microwave Conference (RFM)*, 444–447, 2011.
26. Coulibaly, Y., M. Nedil, L. Talbi, and T. A. Denidni, "Design of mm-wave broadband CPW-fed stacked dielectric resonator antenna for underground mining communication," *IEEE International Symposium on Antennas and Propagation Society*, 1–4, 2010.
27. Kumari, R., K. Parmar, and S. K. Behera, "Conformal patch fed stacked triangular dielectric resonator antenna for WLAN applications," *International Conference on Emerging Trends in Robotics and Communication Technologies (INTERACT)*, 104–107, 2010.
28. Yaduvanshi, R. S. and H. Parthasarathy, *Rectangular Dielectric Resonator Antennas*, Springer, New Delhi, India, 2016.
29. Ding, Y. and K. W. Leung, "On the dual-band DRA-slot hybrid antenna," *IEEE Transactions on Antennas and Propagation*, Vol. 57, No. 3, 624–630, 2009.
30. Lin, Y.-F., H.-M. Chen, and C.-H. Lin, "Compact dual-band hybrid dielectric resonator antenna with radiating slot," *IEEE Antennas and Wireless Propagation Letters*, Vol. 8, 6–9, 2008.
31. Chen, H.-M., Y.-K. Wang, Y.-F. Lin, S.-C. Lin, and S.-C. Pan, "A compact dual-band dielectric resonator antenna using a parasitic slot," *IEEE Antennas and Wireless Propagation Letters*, Vol. 8, 173–176, 2008.
32. Bakshi, G., A. Vaish, and R. S. Yaduvanshi, "Sapphire stacked rectangular dielectric resonator aperture coupled antenna for C-band applications," *Wireless Personal Communications*, Vol. 108, No. 2, 895–905, 2019.
33. Bakshi, G., A. Vaish, and R. S. Yaduvanshi, "Two-layer Sapphire rectangular dielectric resonator antenna for rugged communications," *Progress In Electromagnetics Research Letters*, Vol. 85, 73–80, 2019.
34. Wang, F., et al., "Ultra-wideband dielectric resonator antenna design based on multilayer form," *International Journal of Antennas and Propagation*, Vol. 2019, Article ID 4391474, 2019.
35. Mashhadi, S. H. H., Y.-C. Jiao, and J. Chen, "Broadbeam cylindrical dielectric resonator antenna," *IEEE Access*, Vol. 7, 112653–112661, 2019.
36. Divya, G., K. Jagadeesh Babu, and R. Madhu, "A synoptic review on dielectric resonator antennas," *Microelectronics, Electromagnetics and Telecommunications*, 185–196, Springer, Singapore, 2018.